JOURNAL OF PETROLOGY | VOLUME 47 | NUMBER 5 | PAGES 883–900 | 2006 | doi:10.1093/petrology/egi099

Cotectic Proportions of Olivine and Spinel in Olivine-Tholeiitic Basalt and Evaluation of Pre-Eruptive Processes

PETER ROEDER[1]*, EMMA GOFTON[2] AND CARL THORNBER[3]

[1]DEPARTMENT OF GEOLOGICAL SCIENCES, QUEEN'S UNIVERSITY, KINGSTON, ONT., K7L 3N6, CANADA

[2]DEPARTMENT OF EARTH AND OCEAN SCIENCES, THE UNIVERSITY OF BRITISH COLUMBIA,VANCOUVER, B.C., V6T 1Z4, CANADA

[3]US GEOLOGICAL SURVEY, CASCADES VOLCANO OBSERVATORY, VANCOUVER, WA 98683, USA

RECEIVED APRIL 20, 2005; ACCEPTED DECEMBER 20, 2005
ADVANCE ACCESS PUBLICATION FEBRUARY 13, 2006

The volume %, distribution, texture and composition of coexisting olivine, Cr-spinel and glass has been determined in quenched lava samples from Hawaii, Iceland and mid-oceanic ridges. The volume ratio of olivine to spinel varies from 60 to 2800 and samples with >0·02% spinel have a volume ratio of olivine to spinel of approximately 100. A plot of wt % MgO vs ppm Cr for natural and experimental basaltic glasses suggests that the general trend of the glasses can be explained by the crystallization of a cotectic ratio of olivine to spinel of about 100. One group of samples has an olivine to spinel ratio of approximately 100, with skeletal olivine phenocrysts and small (<50 μm) spinel crystals that tend to be spatially associated with the olivine phenocrysts. The large number of spinel crystals included within olivine phenocrysts is thought to be due to skeletal olivine phenocrysts coming into physical contact with spinel by synneusis during the chaotic conditions of ascent and extrusion. A second group of samples tend to have large olivine phenocrysts relatively free of included spinel, a few large (>100 μm) spinel crystals that show evidence of two stages of growth, and a volume ratio of olivine to spinel of 100 to well over 1000. The olivine and spinel in this group have crystallized more slowly with little physical interaction, and show evidence that they have accumulated in a magma chamber.

KEY WORDS: *olivine; spinel; basalt glass; volume %; cotectic*

INTRODUCTION

Spinel (Cr-spinel and chromite) and olivine are often the first phases to crystallize from basaltic magma containing >6 wt % MgO (Hill & Roeder, 1974; Thy, 1983; Roeder *et al.*, 2001). However, the textural and compositional diversity of spinel and olivine that coexist in basalt is suggestive of variable magmatic conditions. Olivine phenocrysts are one to two orders of magnitude larger in size than spinel microphenocrysts (Fig. 1a) and two to three orders of magnitude greater in volume % than spinel microphenocrysts. Wright (1973) calculated that the volume ratio of olivine to spinel varied from 100 to 150 in a number of samples from the 1959 eruption at Kilauea. The low volume % of spinel and small size of spinel microphenocrysts in basalt is due to the very low solubility of chromium (200–500 ppm Cr) in basaltic melt (Hill & Roeder, 1974). It has been observed (e.g. Wilcox, 1954; Thy, 1983; Roeder *et al.*, 2001) that spinel in lava is often spatially associated with olivine phenocrysts (Fig. 1a), although there have been no published quantitative data on the distribution of spinel between olivine phenocrysts and melt (glass).

Thy (1983) suggested that the spinel–olivine spatial association may be the result of crystallization of olivine causing the nucleation of spinel at the olivine–melt interface, with subsequent incorporation of the spinel in the olivine phenocrysts. Roeder *et al.* (2001), however, suggested that the olivine and spinel may nucleate independently and that the larger olivine phenocrysts incorporate spinel crystals that come into physical contact with olivine during growth under dynamic magmatic conditions. Vogt (1921) introduced the term synnuesis (swimming-together) to describe this process

*Corresponding author. Telephone: (613)533-6185. E-mail: roeder@geol.queensu.ca

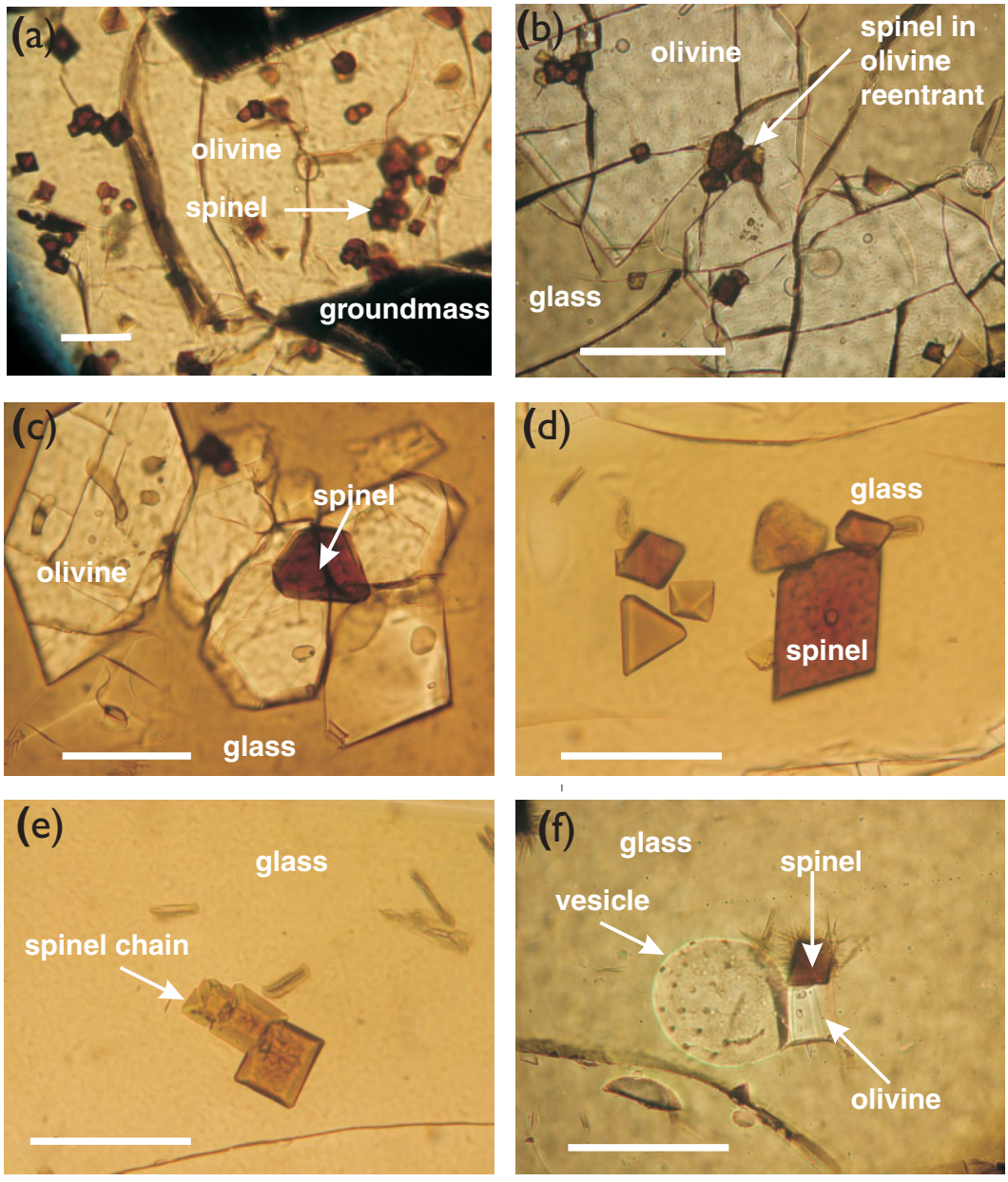

Fig. 1. Spinel octahedra in transmitted light. (a) Olivine with included spinel in crystallized groundmass that appears black, sample AG22-9-2. (b) Reentrant in olivine containing five spinel crystals (arrow). (c) Spinel octahedron in a group of olivine crystals. (d) Spinel octahedra in glass. (e) Chain of three oriented spinel octahedra in glass. (f) Small spinel and olivine attached to a vesicle. Note tiny sulphide blebs on inner surface of vesicle. Scale bar represents 100 μm in all figures except as noted.

and showed in a photomicrograph an example of olivine in dunite that contained a group of approximately 20 chromite octahedra (Vogt, 1921, fig. 1). Synnuesis would explain why groups of spinel crystals are often associated with reentrants within olivine (Fig. 1b, present study) or trapped by groups of olivine crystals (Fig. 1c). The majority of spinel crystals in lava are euhedral octahedra in various orientations relative to the plane of the thin section (Fig. 1d) and often occur well away from olivine phenocrysts. However, some spinel crystals are in chains of oriented octahedra (Fig. 1e) that are independent of olivine, suggesting diffusion-controlled growth (Roeder *et al.*, 2001). Some of the chromite octahedra in Vogt's example (Vogt, 1921, fig. 1) seem to be oriented and thus may be a chain, but the chain plus other chromite octahedra probably came together with olivine by synnuesis. It is also fairly common to find small spinel octahedra that become attached to

vesicles (Fig. 1f) during late-stage vesiculation prior to eruption.

Our approach to evaluating the petrological diversity of coexisting spinel and olivine in basalt entailed a quantitative assessment of the distribution, size, volume %, and composition of coexisting olivine, spinel and glass in naturally quenched samples of olivine-tholeiitic basalt. The measured relative amounts of olivine and spinel in the lavas are compared with the relative amount expected during equilibrium cotectic crystallization. The deviation from cotectic proportions is considered in light of the textural relationship of olivine and spinel in the samples, and what this can tell us about the pre-eruption history of the magma.

SAMPLES

It was a necessary prerequisite that the basalts used in this study had to have been rapidly quenched and thus contain significant glass with >6 wt % MgO along with olivine and spinel, and show little evidence of secondary alteration. The samples that were chosen are shown in groups in Tables 1 and 2. All are olivine normative, as are the glass compositions, except for four quartz-normative glasses indicated by 'Q' in Table 2. The first group of three samples are from Kilauea, Hawaii. Olivine and spinel are the only crystalline phases in these samples. The two Pu'u 'O'o samples (Pu'u 'O'o–Kupaianaha rift-zone eruption) were quenched and collected (Thornber, 2001) on January 22, 1998. Sample 1998S is from vent spatter and sample 1999T (Fig. 2a) is a 'Pele's Tear' sample from tephra. These two Pu'u 'O'o samples are very similar in that they contain glass, olivine phenocrysts and spinel microphenocrysts up to 60 μm in size (Roeder *et al.*, 2003). Some of the olivine phenocrysts are skeletal (Fig. 2b) and include many small spinel crystals (Fig. 2b–d). The highly vesicular sample labeled 1921 is from the 1921 Kilauea summit eruption in the Halemaumau Crater. Experiments were conducted on a portion of this sample by Fudali (1965) and Hill & Roeder (1974).

The second and third group of samples in Tables 1 and 2 are mid-ocean ridge basalt (MORB) samples that were archived at the Woods Hole Oceanographic Laboratory. Each polished thin section shows a gradation from glass at a pillow margin to a devitrified or crystallized pillow interior. The 12 AG22 samples were dredged by the *Argulas* in 1981 from the Southwest Indian Ocean (SWIO) Spreading Zone. It was only discovered after the volume % measurements were completed that seven of the 12 samples were from the same dredge haul (AG22-5) and thus very similar in character. These samples contain plagioclase microphenocrysts and have about 1% euhedral olivine phenocrysts that are up to 400–500 μm in length. The olivine crystals are often in groups of 3–10 crystals (Fig. 3a) with only the rare occurrence of included spinel microphenocrysts (Fig. 3b). Two of the AG22-5 samples contain a single relatively large (100–150 μm) rounded spinel crystal (Fig. 4a and b) that is associated with groups of olivine phenocrysts. These two spinel grains are anomalous because of their size and their rounded shape (Fig. 4d and e). The third group of five SWIO samples shown in Tables 1 and 2 are variable in character. Sample KN54-51-17 from the Mid-Cayman Rise (MCR) was collected by dredging from the R.V. *Knorr* in 1976 (Elthon *et al.*, 1995).

The samples labeled ALV were collected from the Mid-Atlantic Ridge (MAR) using the submersible *Alvin* as part of FAMOUS (French–American Mid-Ocean Undersea Study) as reported by Bryan & Moore (1977). These samples have a higher MgO content in the glasses, and higher calculated temperature (Table 2), than most of the other samples in our study. The olivine crystals shown in Fig. 5a are almost in optical continuity and are interpreted as part of a small mat of olivine cumulate plus a large included spinel (Fig. 5a and b) that was incorporated by the magma at the time of extrusion. The three ALV519 samples have large anhedral olivine phenocrysts (Fig. 5a). Some large spinel crystals have vermiform overgrowths (Fig. 5b and c) where the spinel is in contact with glass but not that portion of spinel incorporated in olivine. This complex vermiform zoning has been described in detail by Roeder *et al.* (2001) and is thought to be the result of diffusion-controlled crystallization.

Sample Mid-P is a hyaloclastite that is thought to have been the product of a sub-glacial eruption in the Western Rift Zone of Iceland (Hardardottir, 1986; Tronnes, 1990; Hansteen, 1991). This sample (Fig. 6) is mainly glass with large anhedral olivine phenocrysts (Fig. 6b) relatively free of included spinel. Some of the large spinel microphenocrysts (Fig. 6c–e) are zoned with a complex vermiform overgrowth.

TECHNIQUES

Measurement of volume %

The volume % olivine in rapidly quenched basalts can be easily determined either by point counting a thin section or by calculation from knowledge of the MgO content of the whole rock, olivine and glass. We have chosen to measure the area of olivine, glass, vesicles and other phases such as plagioclase, pyroxene and sulphide on polished thin sections by using a computer program named Image J that was placed in the public domain by the US National Institutes of Health (Rasband, 2002). This program allowed us to outline the area of the vesicles and various phases using digital photomicrographic images of uncoated polished thin sections.

Table 1: Volume % and distribution of spinel and olivine in basaltic glasses

Sample		Location	Vol. %[1] olivine	Vol. %[1] spinel	No. Sp[2]/cm^2	% No.[3] spinel in olivine	Ol/Sp[4] vol. %	Vol. % Sp[5] (size μm) with olivine	Vol. % Sp[6] (size μm) with glass
Pu'u 'O'o 1998S	I	Kilauea	3·4(3·5)	0·048(·060)	162	45%	70	0·047 (19)(18)	0·0012 (16)(15)
Pu'u 'O'o 1999T	I	Kilauea	3·7	0·042	110	40%	90	0·038 (22)(16)	0·0044 (12)(10)
1921 flow	I	Kilauea	6·3	0·016	77	60%	400	0·014 (15)(12)	0·0021 (11)(11)
AG22-5-7	II	SWIO	1·0	0·0014	9	14%	710	0·0004 (10)	0·0011 (14)
AG22-5-10	II	SWIO	1·2	0·0006	10	—	1900	0·0004 (18)	0·0002 (—)
AG22-5-13	II	SWIO	0·6	0·0004	4	25%	1550	0·0002 (10)	0·0002 (10)
AG22-5-25	II	SWIO	0·8	0·0014	17	12%	550	0·0006 (9)	0·0008 (10)
AG22-5-27	II	SWIO	1·2	0·0004	4	18%	2800	0·0003 (12)	0·0002 (8)
AG22-5-31	II	SWIO	1·4	0·0006[L]	9	29%	2300[L]	0·0002 (7)*[L]	0·0005 (9)
AG22-5-35	II	SWIO	0·9	0·0010[L]	9	35%	910[L]	0·0004 (10)*[L]	0·0006 (12)
AG22-1-6		SWIO	1·4	0·0094	37	22%	140	0·0030 (17)(18)	0·0064 (14)(15)
AG22-7-1		SWIO	4·1	0·022	71	30%	190	0·021 (18)	0·0007 (14)
AG22-7-2		SWIO	2·3	0·013	49	42%	180	0·012 (17)	0·0010 (13)
AG22-8-12		SWIO	NM	0·0003	49	6%	—	0·0003 (16)	0·0001 (13)
AG22-9-2	I	SWIO	4·9	0·051	329	42%	100	0·041 (13)(12)	0·0097 (11)(12)
KN54-51-17		MCR	2·3	0·0092	113	1%	250	0·0064 (9)(9)	0·0028 (9)(9)
ALV519-5-1	II	MAR	3·4	0·042	16	12%	80	0·020 (49)*	0·022 (52)
ALV519-2-1A	II	MAR	2·4	0·041	14	11%	60	0·016 (48)*	0·025 (61)
ALV519-2-1B	II	MAR	1·9	0·012	5	27%	150	0·011 (58)*	0·0012 (26)
ALV520-1-1	II	MAR	6·6(1·2)	0·074(·063)	16	9%	90	0·074 (53)*	0·0005 (32)
ALV528-2-1		MAR	3·8(2·5)	0·014(·060)	55	11%	270	0·011 (20)(15)	0·0031 (10)
ALV529-3-2		MAR	4·7	0·037	102	19%	130	0·031 (20)	0·0063 (17)
Mid-P	II	Iceland	15·5	0·15	127	7%	100	0·096 (46)(42)*	0·056(26)(21)**

[1]Volume % olivine and spinel are reported vesicle free. Number in parenthesis is volume % calculated from XRF analysis of whole rock.
[2]Number of spinel crystals per cm^2 of the thin section vesicle free.
[3]Percentage of number of spinels enclosed in olivine.
[4]Ratio of volume % olivine to volume % spinel.
[5]Volume % spinel associated with olivine. Average size of spinel as measured in reflected light in parenthesis. Underlined average size measured in transmitted light.
[6]Volume % spinel in glass well away from olivine.
*These samples have a spinel >100 μm.
**This average width of 21 μm ($n = 62$) is without one large spinel (Fig. 6c) about 0·5 mm long. If this spinel is included the average is 45 μm ($n = 63$).
[V]Vol. % Sp associated with olivine are spinels either completely enclosed by olivine (Fig. 1a), attached to olivine (Fig. 3b) or within a group of olivine phenocrysts (Fig. 1c).
[U]Measured in transmitted light.
[L]The data for spinel do not include one large (>100 μm) spinel out of the measurement area near the edge of the thin section. of the thin section.
2NM, not measured because of complex olivine–plagioclase intergrowth.

The measurement of the volume % and distribution of spinel microphenocrysts is much more difficult, however, because of the small size of the spinel crystals (~25 μm) and the small amount of spinel, normally <0·05 vol. % (Gofton, 2002).The dimensions of the spinel crystals were estimated directly on the polished thin section using a scale in the microscope eyepiece. The area of the phases was assumed to be proportional to the volume % of the various phases (Chayes, 1956). The volume % of olivine, spinel and glass is calculated relative to a vesicle-free volume. The size of the spinel was measured on the polished surface of the samples, but because many of the spinel crystals are smaller than the thickness of the thin section this measurement may underestimate the actual maximum dimensions of the crystals. The size of the spinel crystals could only be measured in

Table 2: MgO and Cr in glasses

Sample		Location		MgO (wt %)	Cr (ppm)	Temp.[1] (°C)	Log f_{O_2}[2]	Ol-glass K_d[3]
Pu'u 'O'o 1998	I[4]	Kilauea	Q[5]	7·41	362	1180	−9·4	0·26
Pu'u 'O'o 1999	I	Kilauea	Q	7·50	337	1182	−9·2	0·26
1921 flow	I	Kilauea	Q	6·59	270	1156	−9·3	0·26
AG22-5-7	II	SWIO		7·54	305	1184	−8·9	0·25
AG22-5-10	II	SWIO		8·06	283	1194	−8·3	0·28
AG22-5-13	II	SWIO		7·46	296	1181	−8·9	0·24
AG22-5-25	II	SWIO		7·70	296	1190	−8·5	0·26
AG22-5-27	II	SWIO		7·78	273	1190	−9·4	0·24
AG22-5-31	II	SWIO		7·38	308	1187	−9·1	0·24
AG22-5-35	II	SWIO		7·63	295	1187	−8·7	0·25
AG22-1-6		SWIO		7·60	301	1183	−10·0	0·25
AG22-7-1		SWIO		7·47	318	1180	−9·3	0·25
AG22-7-2		SWIO		7·25	308	1174	−9·5	0·23
AG22-8-12		SWIO		6·62	274	1165	−9·6	0·25
AG22-9-2	I	SWIO		7·27	305	1169	−9·5	0·23
KN54-51-17		MCR		6·56	222	1165	−8·5	0·23
ALV519-5-1	II	MAR		9·20	416	1207	−9·1	0·23
ALV519-2-1A	II	MAR		9·29	393	1212	−8·7	0·23
ALV519-2-1B	II	MAR		9·29	393	1212	−8·7	0·23
ALV520-1-1	II	MAR		9·59	409	1215	−8·6	0·23
ALV528-2-1		MAR		9·78	486	1220	−8·7	0·24
ALV529-3-2		MAR	Q	8·66	423	1195	−9·0	0·24
Mid-P	II	Iceland		9·17	380	1201	−9·3	0·23

[1]Temperature calculated using olivine–melt equations of Beattie (1993).
[2]Log f_{O_2} calculated using equations of Poustovetov & Roeder (2001).
[3]K_d for average olivine (core + rim) and average melt composition assuming $Fe^{2+} = 0{\cdot}9 \times$ Fe total for the melt. $K_d = (Mg/Fe^{2+})^{glass}(Fe^{2+}/Mg)^{olivine}$.
[4]I or II signifies sample is in group I or II as explained in the text.
[5]Q signifies that the glass composition is quartz normative as compared with olivine normative for the other samples. The CIPW calculation was from the computer program of K. Hollocher (Union College).

transmitted light for about a third of each sample because the melt at some distance from the melt–seawater contact partially crystallized during quenching (Fig. 4a). This made it impossible to see in transmitted light many of the smaller spinel crystals. The size difference of spinel crystals as measured in reflected and transmitted light is shown for some samples in Table 1. For ease of calculation and comparison, the final average size of the spinel crystals is reported as the side of a square area. The measurement of the area of spinel in a thin section is difficult and very labor intensive because of the small size and small amount of spinel, thus the final values are at best semi-quantitative. It was not possible to measure spinel crystals smaller than about 2 μm using these techniques. The number of spinel crystals varied from only 11 crystals over 2·62 cm^2 of sample (minus vesicles) for sample AG22-5-27 to 661 crystals measured over 2·00 cm^2 of sample AG22-9-2. A total of 3151 spinel crystals were measured. Samples 1998S and 1999T were collected from the Pu'u 'O'o vent on the same day and the volume % and size measurements were made by different operators (the first two authors). The similar results for these two samples in Table 1 are an indication of the reproducibility of the measurements. Although the values of size and volume % are sometimes reported to two significant figures, our level of confidence of the values for spinel below 0·01% is not much better than 100% of their value. The volume % of spinel spatially associated with olivine phenocrysts and the volume % spinel isolated in glass were also measured (see Table 1). Our definition of 'spinel associated with olivine phenocrysts' is spinel that is either completely enclosed

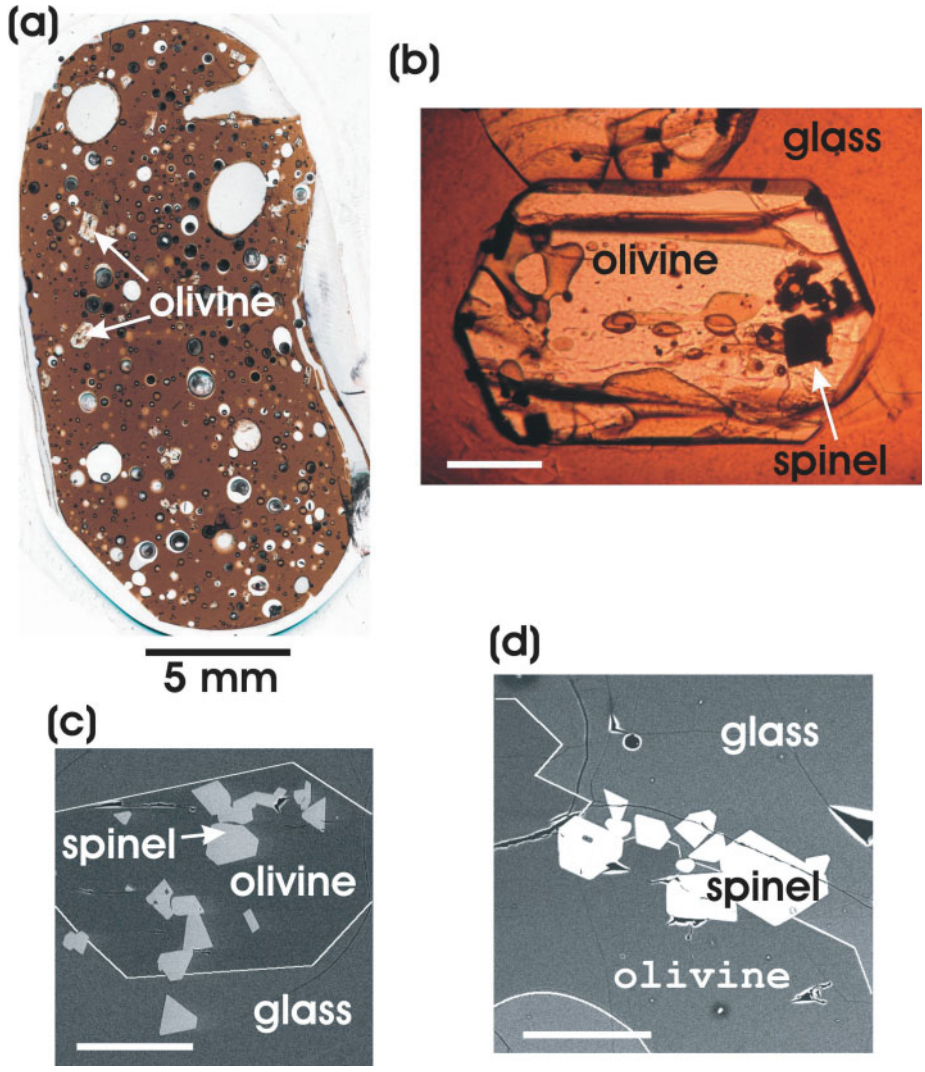

Fig. 2. Kilauea Pu'u 'O'o sample. (a) Polished thin section of sample 1999T in the shape of a tear. (b) Skeletal olivine with included melt inclusions and opaque spinel. (c, d) BSE (back-scattered electron) images of spinel in olivine and glass. White lines added to accentuate the BSE contrast between olivine and glass.

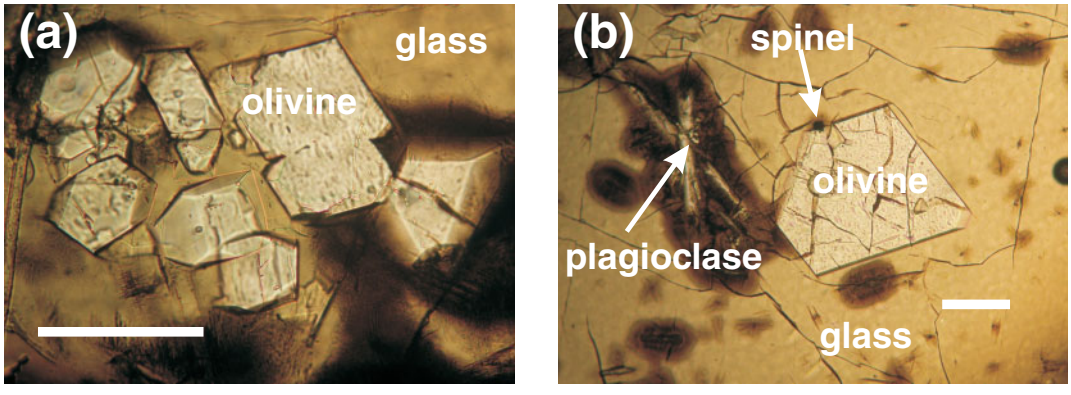

Fig. 3. AG22-5 samples. (a) Group of olivine in partially devitrified glass. (b) Euhedral olivine with small attached spinel plus two prismatic plagioclase crystals surrounded by devitrification.

by olivine (Fig. 1a), within a group of olivine phenocrysts (Fig. 1c) or attached to olivine (Fig. 3b).

Electron microprobe analysis

The glass, olivine and spinel were analyzed by electron microprobe using energy-dispersive analysis as described by Roeder *et al.* (2001). A scanned electron beam (20 μm × 20 μm) was used for the glass analyses and a focused beam for the spinel and olivine analyses. The quality of the analyses was monitored by multiple analyses of three standards that include glass (VG-2 USNM 111240/52), olivine (S-68 analyzed by I. Carmichael, Berkeley) and chromite (USNM117075). The average, standard deviation and listed value for these standards, together with the other analyses, are in an Excel Spreadsheet available for downloading from www.petrology.oxfordjournals.org. The difference between the listed composition and the average ($n = 23$) value for the olivine and for the average (in = 26) chromite can be judged by the filled star and circle-plus sign symbols in Fig. 10. The average ($n = 24$) wt % MgO of the VG-2 glass is 6·58 wt % (SD = 0·14) compared with 6·71 wt % as listed by the Smithsonian Institution.

The chromium values in the basaltic glasses of the present study are all <500 ppm and were measured by wavelength-dispersive analysis with careful attention paid to the background using a technique described by Poustovetov & Roeder (2001). An indication of the accuracy of the technique is that over the 200–500 ppm range of the glasses the results for five standards in this range were within 10% of the listed value (Poustovetov & Roeder, 2001, fig. 2).

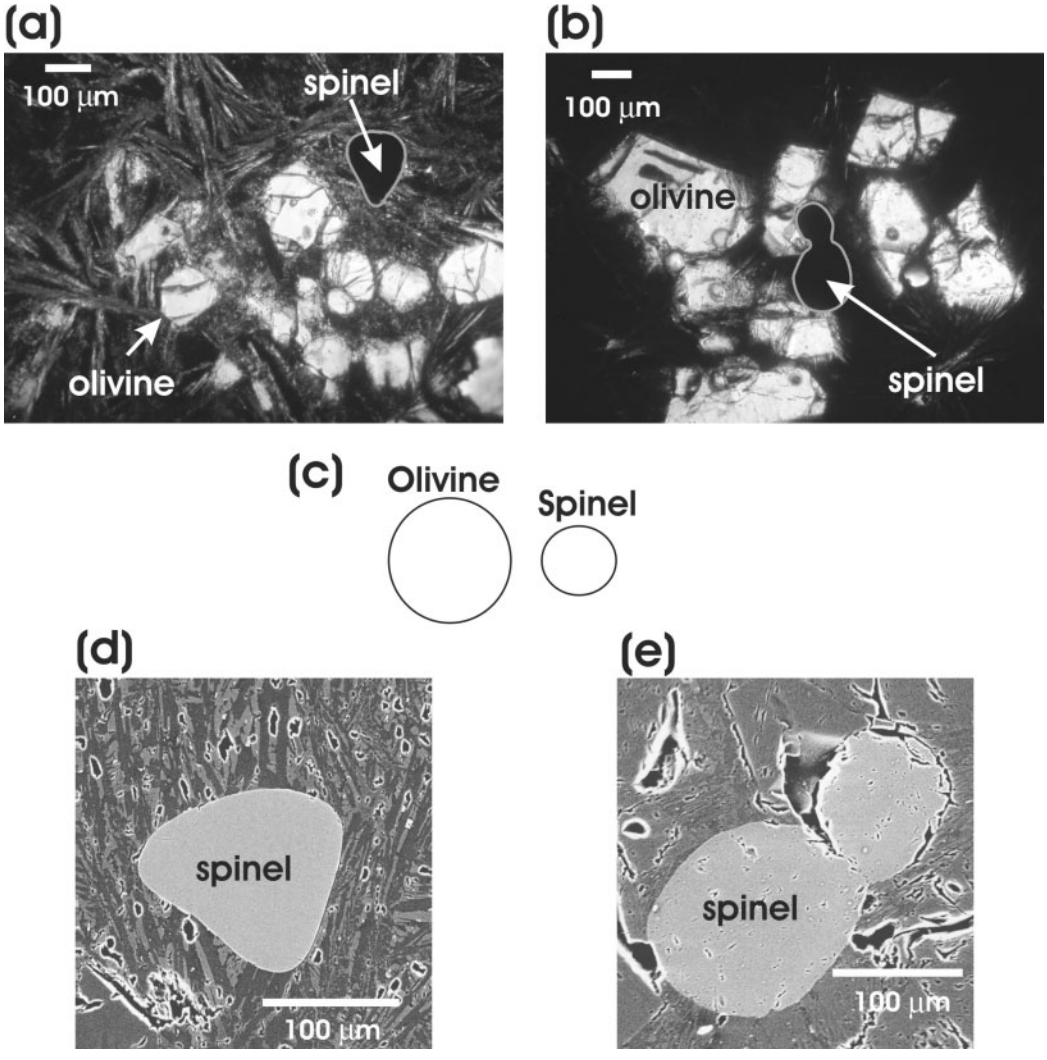

Fig. 4. (a) Group of olivine crystals with spinel outlined in gray. AG22-5-35. (b) Group of olivine crystals with spinel outlined in gray. AG22-5-31. (c) Relative size of olivine (SG = 3·4) and spinel (SG = 5·0) if they settled according to Stokes' Law in a Newtonian melt at equal velocities. (d) BSE image of large anhedral spinel shown in (a). AG22-5-35. (e) BSE image of two anhedral attached spinels shown in (b). AG22-5-31.

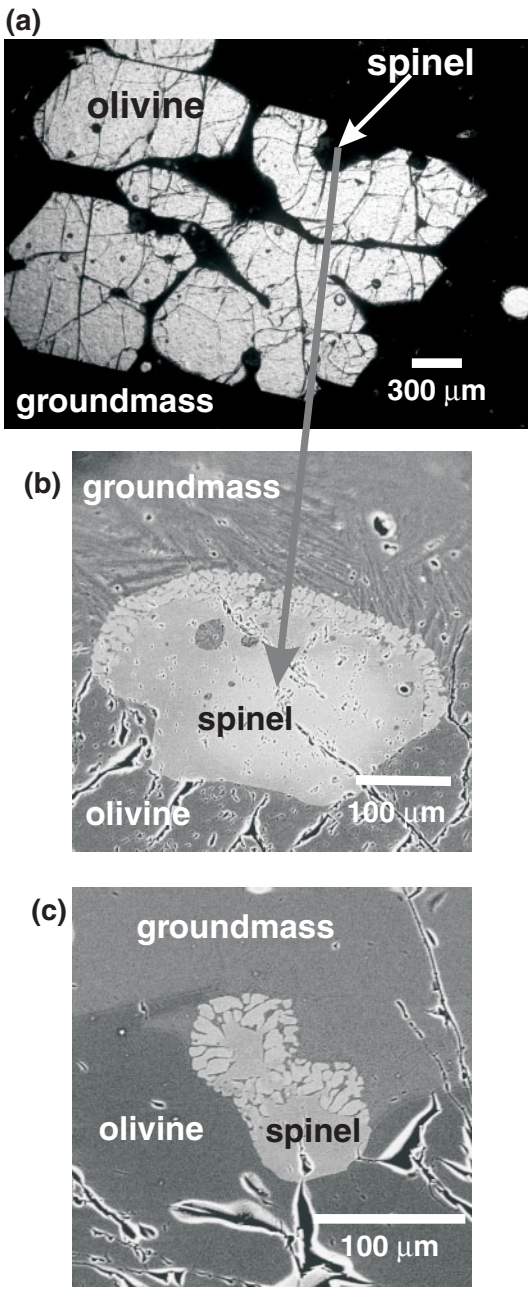

Fig. 5. Sample ALV519. (a) Group of olivine crystals with included spinel in crystallized groundmass. (b) BSE image of spinel partially enclosed in olivine. (c) BSE image of spinel with vermiform rim partially enclosed in olivine.

Temperature and log f_{O_2}

The pre-eruptive temperatures given in Table 2 were calculated using the equations of Beattie (1993) for melt in equilibrium with olivine. The values for log f_{O_2} in Table 2 were calculated using the equations of Poustovetov & Roeder (2001) for melt in equilibrium with spinel.

VOLUME % SPINEL, SIZE OF SPINEL AND GLASS COMPOSITION

The relative volume %, distribution and size of olivine, spinel and glass for 23 thin sections are given in Table 1. The Kilauea samples have a high concentration of spinel per cm^2 (77–162), a high proportion of spinel included within olivine phenocrysts (>40%), a high volume % of spinel associated with olivine phenocrysts and a small average size of spinel (10–22 μm). The largest measured spinel in the three Kilauea samples is 59 μm.

All seven AG22-5 samples from the same SWIO dredge haul (second group in Tables 1 and 2) have a very low volume % spinel (<0·002%), a very low number of spinel crystals (4–17 per cm^2), a low percentage of spinel included within olivine phenocrysts (<40%) and a very small average size (7–18 μm) of spinel with a maximum size of 29 μm. The MgO in the glass for the AG22-5 samples varies from 7·38 to 8·06% and the Cr in the glass is in the range 270–310 ppm. This range of values of Cr is within the estimated analytical error. Calculated temperatures are in the range 1184–1194°C. The similar results for these seven samples leave little doubt that these samples are from the same lava flow and are a demonstration of the reproducibility of the measurements.

The results for the third group of five AG22 samples in Table 1 are variable. The last member of this group, AG22-9-2, has a very high concentration of small spinel grains (329 per cm^2) and a high proportion (42%) of spinel within olivine phenocrysts, both characteristics in common with the Kilauea samples.

The first four of the group of ALV thin sections have relatively high volume % spinel, low % of spinel included in olivine phenocrysts (<30%), a relatively large average size of spinel, and each thin section contains a spinel larger than 100 μm (see asterisk in next to last column of Table 1). Many of the spinel crystals have a vermiform rim where the spinel is in contact with glass. All of the ALV sections have a higher MgO and Cr content in the glass (Table 2) than the Kilauea and SWIO samples, and thus a higher calculated temperature before quenching.

The Icelandic sample (Mid-P) is similar to the first four ALV samples in that it has a very low volume % of spinel associated with large olivine phenocrysts, contains a large spinel (Fig. 6c) and the spinel crystals have vermiform overgrowths where exposed to glass.

Three bulk samples were available for X-ray fluorescence (XRF) analysis. The volume % olivine and spinel for these samples was calculated by using the composition of the whole rock, the glass, the olivine and the average spinel in the samples (see values in parentheses in the third and fourth columns, Table 1). There is general agreement between the calculated and measured

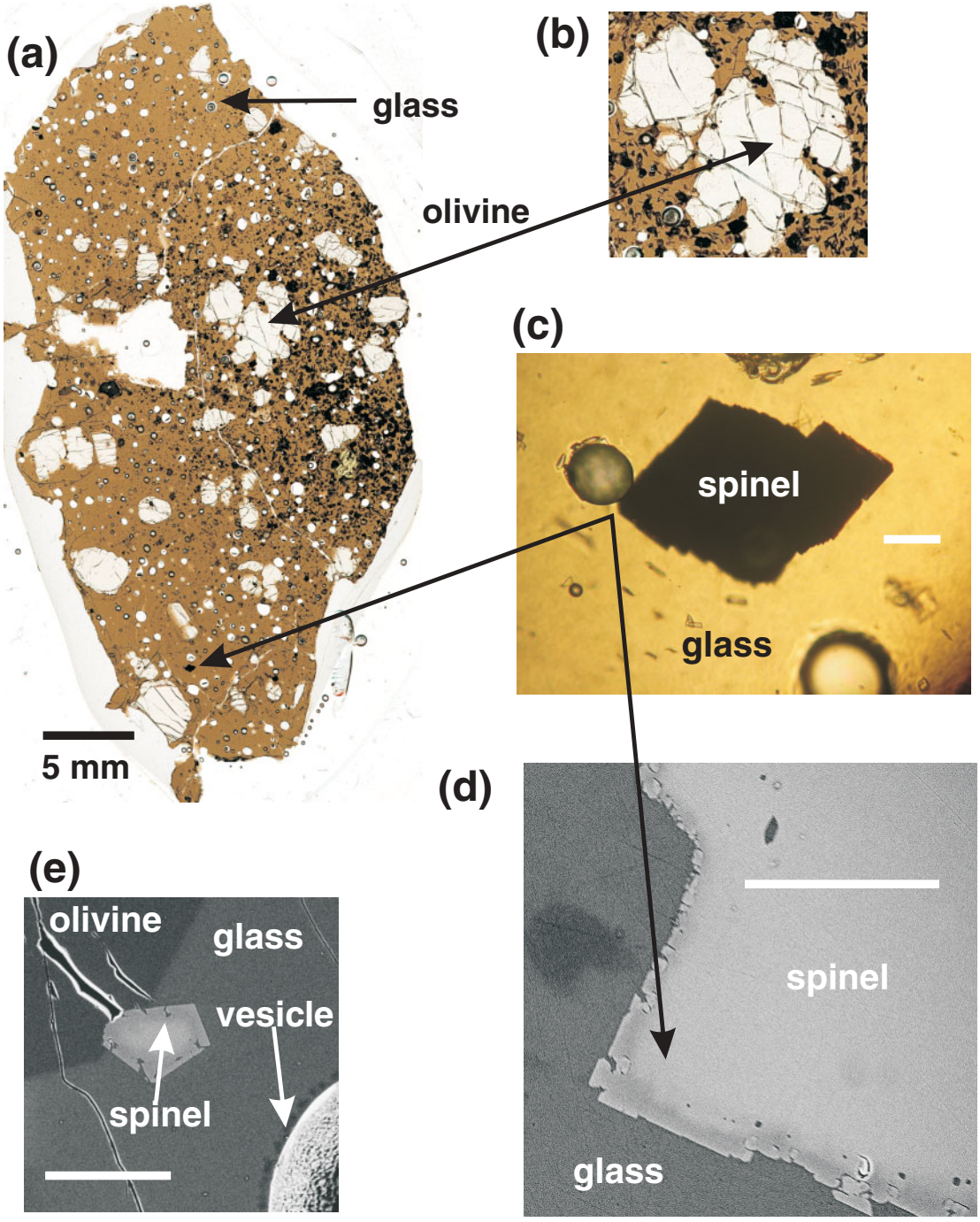

Fig. 6. Iceland sample MID-P. (a) Whole thin section with large irregular olivine crystals in glass. Two arrows connect a spinel shown in (a), (c) and (d). (b) Large irregular olivine (4 mm × 4 mm). (c) Large spinel in glass. (d) BSE image of portion of zoned spinel shown in (a) and (c). (e) BSE image of olivine with attached zoned spinel and vesicle in lower right.

volume % except for a large difference in the value of spinel in sample ALV528 and olivine in ALV520. The most likely explanation for these differences is either heterogeneous distribution of phenocrysts between the polished thin section and the bulk sample analyzed by XRF, or errors in the measurement of volume %. The volume % and composition of the phases for sample AG22-9-2 were used to calculate a whole-rock composition. The calculated results (MgO 9·95%, Cr 561 ppm) compare very favorably with the whole-rock analysis of the same sample (MgO 10·02%, Cr 551 ppm) reported by Mahoney *et al.* (1992).

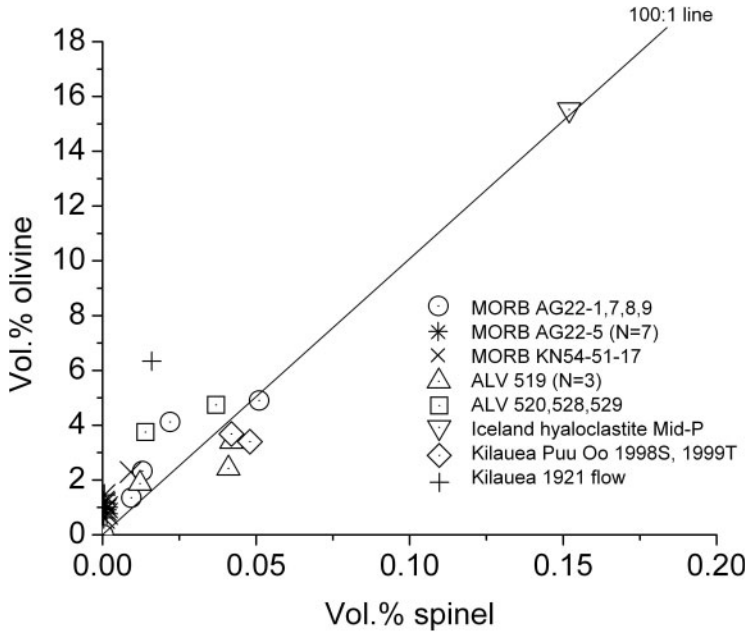

Fig. 7. Volume % olivine vs volume % spinel for 22 samples.

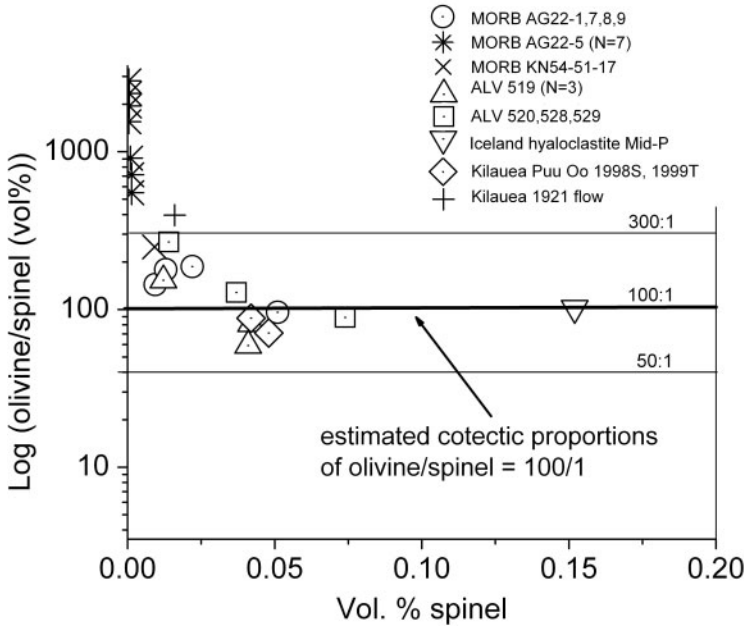

Fig. 8. Logarithm of volume % olivine/volume % spinel vs volume % spinel.

The volume % spinel is plotted vs volume % olivine in Fig. 7. A line representing a 100:1 ratio of olivine to spinel has been added for future reference. Figure 8 is a semi-log plot of the olivine to spinel ratio vs the volume % of spinel and includes lines representing ratios of 300:1, 100:1 and 50:1. Below about 0·02 vol. % spinel the olivine to spinel ratio increases with decreasing volume % spinel. This may reflect a real difference in the ratio or reflect some unknown difficulty in measurement for samples with a very low amount of spinel. It should be noted that the seven AG22-5 samples (asterisks) have very low volume % spinel and thus high olivine to spinel ratios (>500). The volume % measurements were made on a rectangular part of each polished thin section. After the volume % measurements were completed it was discovered that two of the AG22-5 samples (AG22-5-31 and AG22-5-35) contained one large spinel (Fig. 4a and b, d and e) near the edge of the thin section. It

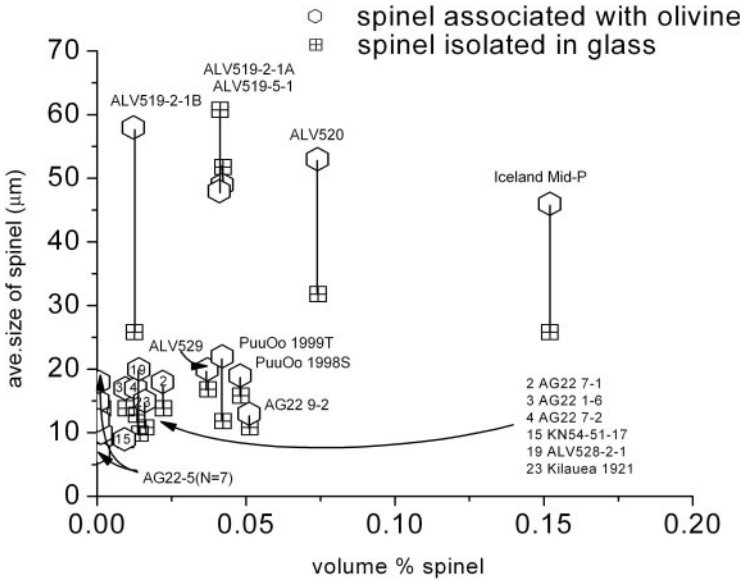

Fig. 9. Average size of spinel associated with olivine connected by a line to the average size of spinel isolated in glass vs volume % spinel for each sample. Sample name or number key is shown for each sample. AG22-5 data do not include the two large spinels found outside the measurement area.

happened that the measurement area that was chosen for volume % measurement did not include these two large spinel crystals. When these crystals are included the average size of spinel and the volume % spinel for these two samples is considerably larger and the olivine to spinel ratio is much lower (188 vs 910 and 287 vs 2300) had they been included. The number of spinel crystals in the measured area for the seven AG22-5 samples was 197 and the largest was 29 μm. This is in contrast to the size (>100 μm) for the two spinel crystals that were outside the area chosen for the volume % measurements. It should be noted that although these two spinel crystals are large by the standard of spinel in lavas they are still very small. The ramifications of the presence of the two large spinel crystals are considered in a subsequent section.

Figure 9 shows the average size, as measured in reflected light, of spinel crystals that are associated with olivine and those isolated in glass plotted versus the volume % of spinel. A tie-line connects the two values. The average size of the spinel associated with olivine is larger than that of the spinel isolated in glass, except for two ALV519 thin sections.

COMPOSITION OF OLIVINE AND SPINEL

Olivine and spinel in 23 thin sections (22 samples) have been analyzed. The complete results of the electron microprobe analyses are available as a supplementary data file, available online at www.petrology.oxfordjournals.org. The $Cr/(Cr + Al)$ vs $Fe^2/(Fe^2 + Mg)$ values for 332 spinel analyses are plotted in the lower part of Fig. 10. The spinel analyses plot in three distinct groups of $Cr/(Cr + Al)$. The three spinel crystals with a $Cr/(Cr + Al)$ of $<0{\cdot}05$, shown at the bottom of Fig. 10, are totally enclosed by olivine phenocrysts, one of which is rounded. It is thought that the olivines that enclose these three spinel grains are exotic wallrock samples that were incorporated by the lava and represent a lower temperature environment. These three spinel analyses were not included in calculations that involved the average spinel composition. The spinel crystals in the MORB samples have $Cr/(Cr + Al)$ values within the range of 0·2–0·6, which is consistent with the results for MORB spinel as reported by Dick & Bullen (1984) and Roeder *et al.* (2001). It should be noted that the spinel crystals from the seven samples (AG22-5) from the same dredge haul all have higher $Fe^2/(Fe^2 + Mg)$ values than the other MORB samples. The spinel crystals from the three Hawaiian samples are higher in both $Cr/(Cr + Al)$ and $Fe^2/(Fe^2 + Mg)$, and have a composition that is consistent with the spinel reported for other samples from Hawaii (e.g. Evans & Moore, 1968; Scowen *et al.*, 1991; Clague *et al.*, 1995; Roeder *et al.*, 2003).

The average $Fe^2/(Fe^2 + Mg)$ values of the olivine in the samples are in the range 0·1–0·2, and are plotted in the top part of Fig. 10 with the scale expanded, to show the individual values. The higher $Fe^2/(Fe^2 + Mg)$ of the olivine in the three Kilauea samples is consistent with the higher $Fe^2/(Fe^2 + Mg)$ of the spinel in these samples. The $Fe^2/(Fe^2 + Mg)$ of the olivine in the seven AG22-5 samples is higher than that of most of the

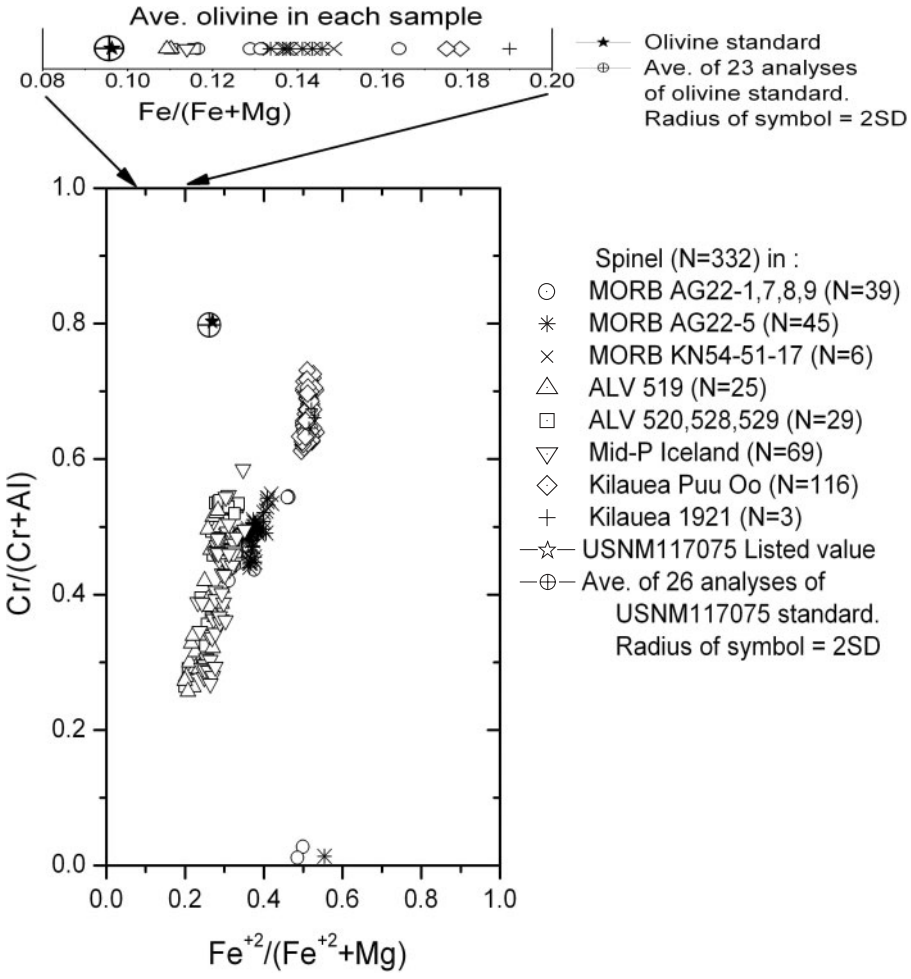

Fig. 10. Cr/(Cr + Al) vs $Fe^2/(Fe^2 + Mg)$ for 332 spinel analyses in the 22 samples. The average $Fe^2/(Fe^2 + Mg)$ of olivine in each sample is shown at the top of the figure. The filled star shows the listed values for the olivine (S-68) and spinel (USNM 117075) secondary standards. The circle with cross is the average of 23 analyses of the olivine and 26 analyses of the spinel secondary standards, and the radius of the symbol is equal to two times the standard deviation.

MORB samples and is consistent with the higher $Fe^2/(Fe^2 + Mg)$ of the spinel in these samples. The most forsteritic olivine are from the ALV samples, which is consistent with the higher calculated liquidus temperature for these samples (Table 2). The average olivine composition and average glass composition were used to calculate a K_d for each sample (Table 2). The K_d values (0·23–0·28) are all less than the expected value of 0·30 (Roeder & Emslie, 1970) because the average olivine composition (core + rim) is more forsteritic than the olivine in equilibrium with melt.

CORRELATION OF VOLUME % OLIVINE AND SPINEL WITH MgO AND Cr CONTENT OF GLASSES

We wish to test the hypothesis that the approximate 100:1 ratio of olivine to spinel found in samples with >0·02 vol. % spinel is close to the cotectic ratio of olivine and spinel that crystallize from basalt with a drop in temperature. The change in the composition of basaltic melts in response to the crystallization of olivine and spinel is best shown on a plot of MgO vs Cr. Figure 11 is a plot of wt % MgO vs ppm Cr in glass for a number of natural and experimental samples that are assumed to contain olivine and spinel. A lower limit of 6 wt % MgO was chosen because experimental evidence (Hill & Roeder, 1974) and evidence from natural samples (Scowen *et al.*, 1991) suggests that spinel may not be a stable phase below about 6 wt % MgO in the melt because of reaction with melt to give pyroxene. The large range of MgO and Cr in Fig. 11 was chosen to include both natural glasses and glasses from 12 experiments on basalts and komatiites. Only those experiments (Murck & Campbell, 1986; Roeder & Reynolds, 1991) that were made at an oxygen fugacity close to the quartz–fayalite–magnetite buffer were

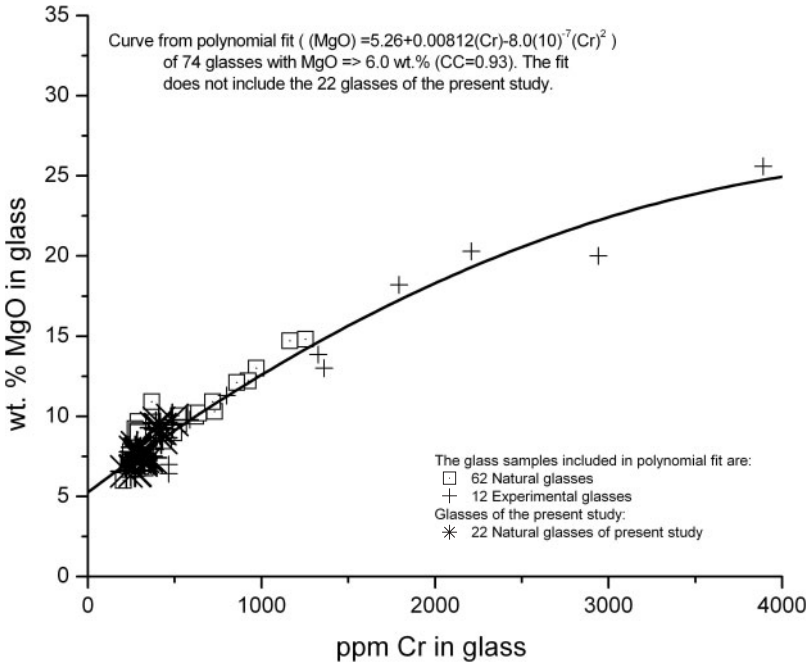

Fig. 11. MgO in glass (wt %) vs Cr in glass (ppm). The curve was calculated by a least-squares fit of 12 experimental glasses (Murck & Campbell, 1986; Roeder & Reynolds, 1991) and 62 natural glasses that include 11 Pu'u 'O'o glasses (Roeder *et al.*, 2003), seven Kilauea Iki glasses (Scowen *et al.*, 1991, and unpublished data), 17 Hawaiian glasses (Wagner *et al.*, 1998), three Iceland and MORB glasses (Roeder *et al.*, 2001) and 24 Blanco Trough glasses (Gaetani *et al.*, 1995).

chosen. This minimizes the effect that a variation in oxygen fugacity has on the Cr content of glasses in equilibrium with spinel as reported by Hill & Roeder (1974) and Berry & O'Neil (2004). The continuous curve is a polynomial fit to those natural (open squares) and experimental glasses (+ symbols) shown in Fig. 11. This polynomial fit does not include the 22 glasses of the present study (asterisks), to allow independent comparison of the results for these 22 glasses with the polynomial fit. The polynomial fit shows a strong positive correlation (correlation coefficient = 0·93) between MgO and Cr for the 74 natural and experimental glasses. This correlation is believed to reflect the change in melt composition as a result of the crystallization of olivine and spinel as a function of decreasing temperature.

It has been demonstrated (i.e. Presnall, 1969; Morse, 1980; Morse *et al.*, 2004) that on a ternary liquidus diagram, the tangent to a cotectic liquidus curve can be used to determine the ratio of solid phases that crystallize at equilibrium at any temperature along the cotectic curve. The curvature of the cotectic curve is a function of the changing ratio of crystalline phases. Irvine (1974) used this to some advantage in describing the liquidus in the $MgCr_2O_4$–Mg_2SiO_4–SiO_2 system and estimating the changing ratio of olivine (forsterite) to spinel (magnesiochromite) for liquid compositions on the cotectic curve. The curvature of that cotectic suggests an increasing ratio of olivine to spinel as the temperature is lowered. Irvine reported that the value of this ratio was close to 100 (weight ratio of 99 or a volume ratio of 143) at a temperature just above the reaction point (peritectic) where magnesiochromite reacts with melt to give pyroxene.

The polynomial curve in Fig. 11 can also be considered to be a cotectic curve for olivine and spinel in mafic and ultramafic magmas. This curve, however, is much more complex than the cotectic curve in the three-component $MgCr_2O_4$–Mg_2SiO_4–SiO_2 system because it combines a range of melt compositions and a range of composition of both olivine and spinel. It is thus surprising how well the data plotted in Fig. 11 conform to a relatively simple relationship. This was shown by Barnes (1998) for ultramafic magmas containing >15 wt % MgO. The curvature of the cotectic shown in Fig. 11 is a complex function of both changing crystal composition and the relative amounts of the crystalline phases. The increasing slope of this curve with decreasing MgO is consistent with the crystallization of an increasing ratio of olivine to spinel with decreasing temperature. The exact ratio can only be determined if the composition of the olivine and spinel is known.

The composition of the glass for the 22 basalts of the present study is re-plotted in Fig. 12 over a much narrower range of MgO and Cr content than shown in Fig. 11. The polynomial curve of Fig. 11 is also included in Fig. 12. Associated with each point in Fig. 12 is a

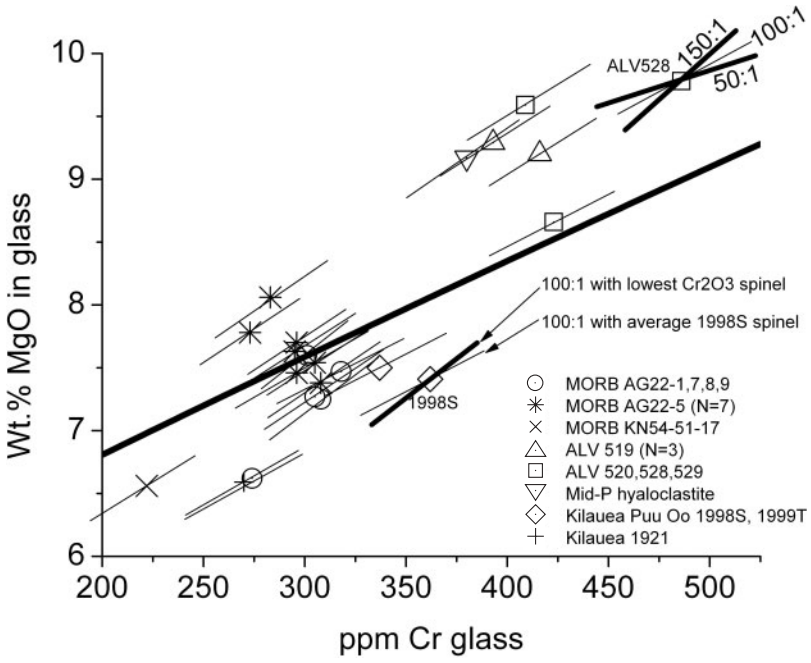

Fig. 12. MgO in glass (wt %) vs Cr in glass (ppm) for the 22 samples of the present study. The fine straight line through each point shows how the composition of the glass changes by the addition or subtraction of the olivine and spinel analyzed for each sample in a ratio of olivine to spinel of 100:1. The bold line is part of the polynomial curve shown in Fig. 11. The three straight lines shown for the sample point ALV528 indicate how the composition would change as the olivine to spinel ratio is changed from 150:1 to 50:1.

straight-line segment that represents the change in MgO and Cr of each melt if a 100:1 volume ratio of the average composition of olivine and spinel found for that sample is either added to or subtracted from that melt. Three line segments are drawn for glass ALV528 to demonstrate the sensitivity of the slope to a varying volume ratio of olivine to spinel of 150:1, 100:1 and 50:1. Also shown are two line segments for sample 1998S to demonstrate the sensitivity of the slope with varying spinel composition. The fine line was calculated assuming the average spinel composition (42·75 wt % Cr_2O_3) found in the 1998S sample whereas the bold line was calculated using the average spinel with the lowest average Cr_2O_3 of all 22 samples (26·15 wt % Cr_2O_3 of AG22-5-27). The slopes of the line segments are relatively insensitive to the narrow range of olivine composition for the 22 samples. The slopes of the fine-line segments are very close to the slope of the independently developed polynomial curve.

We conclude that for most basalts an approximate 100:1 volume ratio of olivine to spinel is consistent with cotectic proportions. The volume ratios of olivine to spinel that were measured in the present study (Fig. 8 and third from right column in Table 1) show a large range but the ratios for those samples having >0·02% spinel are consistent with crystallization of the cotectic proportions of approximately 100:1. The very large ratios for some samples, such as the seven samples of the AG22-5 dredge haul, are due to either measurement problems or a geological process that selectively adds olivine or removes spinel from the magma.

In Fig. 13 the MgO and Cr contents of glasses are compared with the bulk composition of basaltic rocks. Three straight lines that radiate from the glass composition of sample ALV529 (+ symbol) have been drawn to demonstrate the effect of adding to a glass that lies on the curve the ratios of 300:1, 100:1 and 50:1 of olivine to spinel. The majority of glass (blue squares) and rock samples (green circles) with <10% MgO lie close to the so-called polynomial cotectic curve whereas those rock samples with >10% MgO (green circles) follow an approximately linear trend that deviates from the trend of the glasses (blue squares). This suggests that many of the volcanic rocks involved an addition of olivine and spinel in a ratio larger than the cotectic ratio of 100:1, presumably by accumulation of olivine phenocrysts with or without accompanying spinel microphenocrysts. It should be noted that if the olivine to spinel ratio is 100:1 for the bulk sample then the olivine to spinel ratio for the olivine phenocrysts has to be >100, as many spinel crystals are isolated in the glass. Let us consider an example where olivine phenocrysts and spinel crystallized in a cotectic ratio of 100:1 in a quiescent magmatic environment with the volume % spinel divided equally between olivine and melt. The total sample would

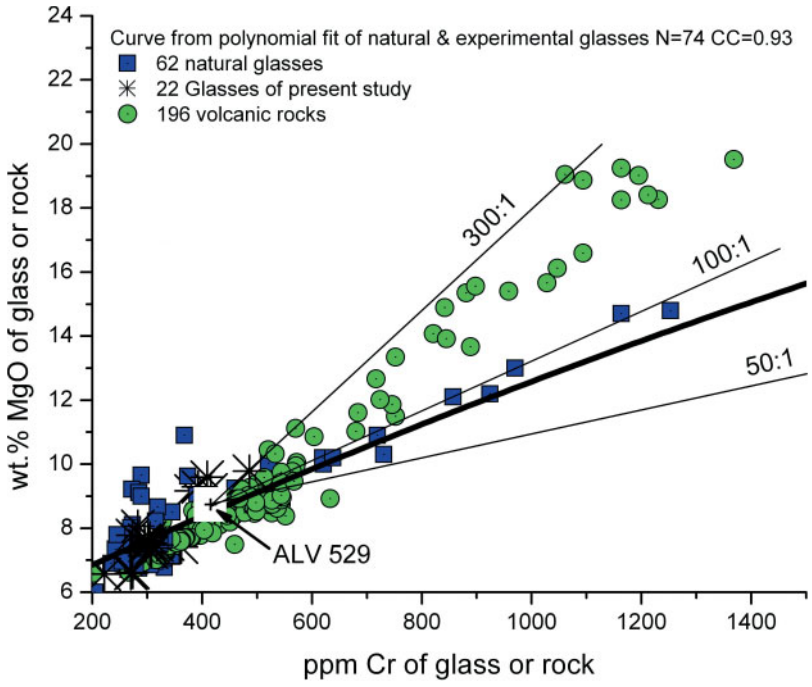

Fig. 13. MgO (wt %) vs Cr (ppm) for the glasses of the present study (asterisks), natural glasses from other volcanic rocks (blue squares) as listed in Fig. 11 caption, and for the bulk composition of volcanic rocks (green circles) from Wright (1973), Garcia *et al.* (1992, 1996) and Clague *et al.* (1995). The bold curve is the same as shown in Figs 11 and 12. The three straight lines show how sample glass ALV529 would change by the addition of olivine to spinel ratios of 300:1, 100:1 and 50:1.

have a cotectic ratio of 100:1 whereas the phenocrysts would have an olivine to spinel ratio of 200:1. If these olivine phenocrysts were then added by crystal settling to a magma with cotectic proportions of olivine and spinel this magma would then lie on the 200:1 line relative to the melt composition. Thus rocks that contain added phenocrysts plus included spinel should always lie above the cotectic ratio of olivine to spinel. This can be used to distinguish volcanic rocks that crystallized from a melt composition from those rocks that have added olivine phenocrysts plus enclosed spinel microphenocrysts. Barnes (1998), in a very neat study, showed the relationship between the so-called olivine–spinel cotectic curve for komatiites and the bulk composition of komatiites. Barnes was able to demonstrate that komatiites with >25% MgO may be undersaturated with respect to chromite.

RELATIONSHIP OF SPINEL TO OLIVINE

The volume % spinel, the distribution of spinel and the size of spinel vary greatly between the samples of basalt. We believe, however, that some of the samples can be separated into two broadly identifiable groups that are identified as I or II in the Sample column of Tables 1 and 2. Group I samples (1998S, 1999T, 1921, AG22-9-2) have a very large number of euhedral spinel crystals, all smaller than 60 μm, with a large percentage of spinel (>40%) included within olivine phenocrysts that are sometimes skeletal. The calculated number of spinel per cm^3 of melt is very high and varies from about 60 000 to 300 000. The olivine to spinel ratio for samples in this group is close to the estimated cotectic ratio of 100:1. We suggest that the olivine and spinel of this group crystallized relatively rapidly under fairly chaotic conditions during ascent and flow of the magma. The relatively rapid growth gave rise to skeletal olivine and the chaotic conditions led to significant olivine—spinel physical interaction. The relative motion of the large olivine phenocrysts and the huge number of very small spinel microphenocrysts led to the incorporation in olivine of the slightly larger spinel microphenocrysts, thus concentrating the smaller spinel crystals in the melt. It is also possible that the smaller spinel crystals in the glass nucleated later than the spinel crystals enclosed within olivine. Another indication of fairly rapid spinel growth in these samples is the presence of spinel chains.

The group II samples (ALV519, ALV520, MID-P, 7 samples of AG22-5) contain olivine phenocrysts that are relatively free of included spinel and the samples often contain a few significantly larger spinel crystals (>100 μm). The calculated concentrations of spinel per cm^3 of melt are lower (<20 000) for the group II samples.

We believe that some of the olivine and spinel crystallized more slowly under quiescent conditions with much less olivine–spinel interaction during growth. Some of the olivine and spinel crystallized well before extrusion and may have been part of a settled sediment layer of olivine and spinel near the base of a magma chamber. A portion of the sediment layer may have been ultimately swept up during the extrusion event. The spinel crystals in some (ALV519, ALV520, Mid-P) of the higher temperature samples have a distinct anhedral core surrounded by a vermiform rim where the spinel was exposed to melt. This is evidence of two distinct stages of growth. The cores of these spinel crystals have higher Cr/(Cr + Al) whereas the vermiform rim is often zoned to lower Cr/(Cr + Al). Spinel with vermiform rims has previously been described (Dick & Bryan, 1978; Graham *et al.*, 1979; Fisk & Bence, 1980; Allan *et al.*, 1988, 1996; Natland, 1989) as a reaction texture, possibly caused by decompression. Roeder *et al.* (2001) described this texture as due to 'the breakdown of the relatively smooth interface between chromian spinel and melt to a type of cellular growth because diffusion in the melt is no longer able to support growth of a smooth interface'. This cellular growth probably represents a major increase in growth rate because of supercooling, and thus diffusion-controlled crystallization caused Cr depletion in the nearby melt, which led to Al-rich rims (Fig. 6d and e).

The AG22-5 samples from the same dredge haul have groups of olivine phenocrysts that are almost completely free of included spinel as well as a low number of small euhedral spinel crystals and thus belong to group II. Two of the samples contain a large (>100 μm) anhedral spinel crystal that is included with a group of olivine crystals (Fig. 4a and b). The calculated concentration of spinel in the melt is 4000–14 000 per cm^3, only about a tenth that of samples in group I. Figure 4c shows the calculated relative size of olivine and spinel assuming they had settled at equal velocity according to Stokes' Law. We suggest that a new magma pulse picked up groups of settled olivine that in two cases included a large anhedral spinel. The magma was extruded relatively quietly on the ocean floor with little new olivine or spinel nucleation and growth. The very high olivine to spinel ratio for these seven samples may be because the olivine phenocrysts are free of included spinel, and some spinel crystals were left behind. We suggest that in most magma chambers where olivine and spinel crystallize contemporaneously, the olivine and spinel tend to crystallize independently, thus giving rise to olivine relatively free of included spinel. It has been observed that where olivine and spinel (chromite) occur together in large layered intrusions such as the Muskox (Roach *et al.*, 1998) and the Jimberlana (Roeder & Campbell, 1985) the olivine crystals are relatively free of included spinel. This may also be due to textural maturation and expulsion during recrystallization.

CONCLUSIONS

The volume % and distribution of olivine, spinel and glass has been measured in 22 rapidly quenched basaltic lavas. The maximum volume % of spinel is 0·15% and the average size of spinel is in the range 10–60 μm, measured as the side of a cube. The majority of the spinel is associated with olivine phenocrysts and these spinels tend to be larger than spinel found isolated in glass. The calculated number of spinel crystals in the melt is enormous and ranges from thousands to hundreds of thousands of crystals per cm^3 of melt. For example, if it is assumed that there is 0·02 vol. % spinel in a sample, the number of calculated spinel crystals per cm^3 of melt varies from 1600 for 50 μm spinel to 200 000 for 10 μm spinel. The ratio of vol. % olivine to spinel for the 22 samples varies from 60 to 2800 and those samples containing >0·02 vol. % spinel tend to have olivine to spinel ratios of approximately 100.

The composition of olivine, spinel and glass in the 22 samples has been determined. A plot of MgO vs Cr in the 22 glasses has been compared with that of glasses from experiments made near the quartz–fayalite–magnetite buffer and with that of a number of other natural basaltic glasses. There is a positive correlation between Cr and MgO in the natural and experimental glasses, which can be explained by the co-crystallization of olivine and spinel in a ratio of approximately 100:1, with the ratio increasing slightly with lowering temperature. Thus it is concluded that those samples with an olivine to spinel ratio of approximately 100:1 crystallized olivine and spinel in approximately cotectic proportions. A plot of MgO vs Cr for volcanic rocks, as compared with volcanic glasses, shows a marked deviation from the so-called cotectic curve above about 10% MgO, which suggests that many of the volcanic rocks do not reflect melt compositions but melt plus added olivine + spinel phenocrysts.

The relative distribution and amount of olivine and spinel can be used to give valuable information on pre-eruptive conditions. It was found that many of the samples could be divided into two discernible groups. One group had spinel with an average size of 25 μm and maximum size of spinel of about 50 μm, >40% of the spinel included within olivine phenocrysts, and an olivine to spinel ratio of approximately 100. It is concluded that the olivine and spinel in this group crystallized during the chaotic conditions during extrusion. These conditions promoted the skeletal growth of olivine, which facilitated the inclusion by synneusis of the tiny spinel crystals within the much larger olivine phenocrysts. The second discernible group includes

those samples where there are few spinel crystals included within olivine phenocrysts, a larger size of spinel with some >100 μm, some spinel with vermiform overgrowths, and olivine to spinel ratios that are sometimes very high. This second group of samples is thought to have partially crystallized under more stable conditions where both olivine and spinel crystallized with little physical interaction under the relatively quiescent conditions within a magma chamber. Some samples in this second group contained groups of olivine crystals that may have been part of a mat of crystals that settled within a magma chamber. It is suggested that the magma upon extrusion picked up both olivine and spinel from the floor of the chamber, but not necessarily in cotectic proportions. The vermiform and zoned rims on spinel in the higher temperature samples reflect a second stage of growth of spinel that occurred upon supercooling during the extrusion event.

ACKNOWLEDGEMENTS

We thank David Kempson for help with the use of the electron microprobe, Robert Renaud for assistance with computing facilities, and Jerzy Advent for thin-section preparation at Queen's University. We particularly wish to acknowledge the help of Henry Dick of the Woods Hole Oceanographic Institution for his assistance in choosing and lending samples for this study. We also acknowledge the late E. F. Osborn for the 1921 Kilauea sample, and thank Nils Oskarsson of the Nordic Volcanological Institute of Iceland for the Icelandic sample, and members of the Woods Hole Oceanographic Institution and members of the US Geological Survey at the Hawaiian Volcano Observatory for their assistance in the collection and preparation of the samples. Heather Jamieson of Queen's University is thanked for her suggestions. Michelle Coombs and Michael Clynne of the US Geological Survey are gratefully acknowledged for their very constructive comments on an early version of the manuscript. We also appreciate the very constructive reviews of Steve Barnes (CSIRO, Australia) and Michael Rhodes (University of Massachusetts).

REFERENCES

Allan, J. F., Sack, R. O. & Batiza, R. (1988). Cr-rich spinels as petrogenetic indicators: MORB-type lavas from the Lamont Seamount Chain, eastern Pacific. *American Mineralogist* **73**, 741–753.

Allan, J. F., Falloon, T., Pedersen, S. B., Lakkapragada, B. S., Natland, J. H. & Malpas, J. (1996). Petrology of selected Leg 147 basaltic lavas and dikes. *Proceedings of the Ocean Drilling Program* **147**, 173–186.

Barnes, S. J. (1998). Chromite in komatiites, 1. Magmatic controls on crystallization and composition. *Journal of Petrology* **39**, 1689–1720.

Beattie, P. (1993). Olivine–melt and orthopyroxene–melt equilibria. *Contributions to Mineralogy and Petrology* **115**, 103–111.

Berry, A. J. & O'Neil, H. St. C. (2004). A XANES determination of the oxidation state of chromium in silicate glasses. *American Mineralogist* **89**, 790–798.

Bryan, W. B. & Moore, J. G. (1977). Compositional variations of young basalts in the Mid-Atlantic Ridge rift valley near lat 36°49′N. *Geological Society of America Bulletin* **88**, 556–570.

Chayes, F. (1956). *Petrographic Modal Analysis; an Elementary Statistical Appraisal*. John Wiley, New York, 113 pp.

Clague, D. A., Moore, J. G., Dixon, J. E. & Friesen, W. B. (1995). Petrology of submarine lavas from Kilauea's Puna Ridge, Hawaii. *Journal of Petrology* **36**, 299–349.

Dick, H. J. B. & Bryan, W. B. (1978). Variation of basalt phenocryst mineralogy and rock compositions in DSDP Hole 396B. In: *Initial Reports of the Deep Sea Drilling Project, 4*. Washington, DC: US Government Printing Office, pp. 215–225.

Dick, H. J. B. & Bullen, T. (1984). Chromian spinel as a petrogenetic indicator in abyssal and alpine-type peridotites and spatially associated lavas. *Contributions to Mineralogy and Petrology* **86**, 54–76.

Elthon, D., Ross, D. K. & Meen, J. K. (1995). Compositional variations of basaltic glasses from the Mid-Cayman Rise spreading center. *Journal of Geophysical Research* **100**, 12497–12512.

Evans, B. W. & Moore, J. G. (1968). Mineralogy as a function of depth in the prehistoric Makaopuhi tholeiitic lava lake, Hawaii. *Contributions to Mineralogy and Petrology* **17**, 85–115.

Fisk, M. R. & Bence, A. E. (1980). Experimental crystallization of chromite spinel in FAMOUS basalt 527-1-1. *Earth and Planetary Science Letters* **48**, 111–123.

Fudali, R. F. (1965). Oxygen fugacities of basaltic and andesitic lavas. *Geochimica et Cosmochimica Acta* **29**, 1063–1075.

Gaetani, G. A., DeLong, S. E. & Wark, D. A. (1995). Petrogenesis of basalts from the Blanco Trough, northeast Pacific: inferences for off-axis melt generation. *Journal of Geophysical Research* **100**, 4197–4214.

Garcia, M. O., Rhodes, J. M., Wolfe, E. W., Ulrich, G. E. & Ho, R. A. (1992). Petrology of lavas from episodes 2–47 of the Puu Oo eruption of Kilauea Volcano, Hawaii: evaluation of magmatic processes. *Bulletin of Volcanology* **55**, 1–16.

Garcia, M. O., Rhodes, J. M., Trusdell, F. A. & Pietruszka, A. J. (1996). Petrology of lavas from the Pu'u 'O'o eruption of Kilauea Volcano: III. The Kupaianha episode (1986–1992). *Bulletin of Volcanology* **58**, 359–379.

Gofton, E. (2002). The association of chromian spinel and olivine in basaltic melts. B.Sc. thesis, Queen's University, Kingston, Ont.

Graham, A. L., Symes, R. F., Bevan, J. C. & Din, V. K. (1979). Chromium-bearing spinels in some rocks of Leg 45: phase chemistry, zoning and relation to host basalt chemistry. In: *Initial Reports of the Deep Sea Drilling Project, 45*. Washington, DC: US Government Printing Office, pp. 581–586.

Hansteen, T. H. (1991). Multi-stage evolution of the picritic Maelifell rocks, SW Iceland: constraints from mineralogy and inclusions of glass and fluid in olivine. *Contributions to Mineralogy and Petrology* **109**, 225–239.

Hardardottir, V. (1986). The petrology of the Maelifell picritic basalt, southern Iceland. *Jokull* **36**, 31–40.

Hill, R. & Roeder, P. L. (1974). The crystallization of spinel from basaltic liquid as a function of oxygen fugacity. *Journal of Geology* **82**, 709–729.

Irvine, T. N. (1974). Chromitite layers in stratiform intrusions. *Carnegie Institution of Washington Yearbook* **73**, 300–316.

Mahoney, J., le Roux, A. P., Peng, Z., Fisher, R. L. & Natland, J. H. (1992). Southwestern limits of Indian Ocean Ridge mantle and the origin of low $^{206}Pb/^{204}Pb$ mid-ocean ridge basalt: isotope systematics

of the central Southwest Indian Ridge (17°–50°E). *Journal of Geophysical Research* **97**, 19771–19790.

Morse, S. A. (1980). *Basalts and Phase Diagrams*. New York: Springer, 493 pp.

Morse, S. A., Brady, J. B. & Sporleder, B. A. (2004). Experimental petrology of the Kiglapait Intrusion: cotectic trace for the Lower Zone at 5 kbar in graphite. *Journal of Petrology* **45**, 2225–2259.

Murck, B. W. & Campbell, I. H. (1986). The effects of temperature, oxygen fugacity and melt composition on the behaviour of chromium in basic and ultrabasic melts. *Geochimica et Cosmochimica Acta* **50**, 1871–1887.

Natland, J. H. (1989). Partial melting of a lithologically heterogeneous mantle: inferences from crystallization histories of magnesian abyssal tholeiites from the Siqueiros Fracture Zone. In: Sanders, A. D. & Norry, M. J. (eds) *Magmatism in the Ocean Basins*. Geological Society, London, Special Publications **42**, 41–70.

Poustovetov, A. A. & Roeder, P. L. (2001). The distribution of Cr between basaltic melt and chromian spinel as an oxygen geobarometer. *Canadian Mineralogist* **39**, 309–317.

Presnall, D. C. (1969). The geometrical analysis of partial fusion. *American Journal of Science* **267**, 1178–1194.

Rasband, W. (2002). ImageJ v1.22d software in public domain. US National Institutes of Health.

Roach, T. A., Roeder, P. L. & Hulbert, L. J. (1998). Composition of chromite in the upper chromitite, Muskox layered intrusion, Northwest Territories. *Canadian Mineralogist* **36**, 117–135.

Roeder, P. L. & Campbell, I. H. (1985). The effect of postcumulus reactions on composition of chrome-spinels from the Jimberlana intrusion. *Journal of Petrology* **26**, 763–786.

Roeder, P. L. & Emslie, R. F. (1970). Olivine–liquid equilibrium. *Contributions to Mineralogy and Petrology* **29**, 275–289.

Roeder, P. L. & Reynolds, I. (1991). Crystallization of chromite and chromium solubility in basaltic melts. *Journal of Petrology* **32**, 909–934.

Roeder, P. L., Poustovetov, A. & Oskarsson, N. (2001). Growth forms and composition of chromian spinel in MORB magma: diffusion-controlled crystallization of chromian spinel. *Canadian Mineralogist* **39**, 397–416.

Roeder, P. L., Thornber, C., Poustovetov, A. & Grant, A. (2003). Morphology and composition of spinel in Pu'u 'O'o lava (1996–1998), Kilauea volcano, Hawaii. *Journal of Volcanology and Geothermal Research* **123**, 245–265.

Scowen, P., Roeder, P. L. & Helz, R. (1991). Reequilibration of chromite within Kilauea Iki lava lake, Hawaii. *Contributions to Mineralogy and Petrology* **107**, 8–20.

Thornber, C. R. (2001). Olivine–liquid relations of lava erupted by Kilauea volcano from 1994–1998: implications for shallow magmatic processes associated with the ongoing east-rift-zone eruption. *Canadian Mineralogist* **39**, 239–266.

Thy, P. (1983). Spinel minerals in transitional and alkali basaltic glasses from Iceland. *Contributions to Mineralogy and Petrology* **83**, 141–149.

Tronnes, R. G. (1990). Basaltic melt evolution of the Hengill volcanic system, SW Iceland, and evidence for clinopyroxene assimilation in primitive tholeitic magmas. *Journal of Geophysical Research* **95**, 15893–15910.

Vogt, J. H. L. (1921). The physical chemistry of the crystallization and magmatic differentiation of igneous rocks. *Journal of Geology* **29**, 318–350.

Wagner, T. P., Clague, D. A., Hauri, E. H. & Grove, T. L. (1998). Trace element abundances of high-MgO glasses from Kilauea, Mauna Loa and Haleakala volcanoes, Hawaii. *Contributions to Mineralogy and Petrology* **131**, 13–21.

Wilcox, R. E. (1954). Petrology of Paricutin volcano, Mexico. *US Geological Survey Bulletin* **965-C**, 281–353.

Wright, T. L. (1973). Magma mixing as illustrated by the 1959 eruption, Kilauea volcano, Hawaii. *Geological Society of America Bulletin* **84**, 849–858.